

Characterization of the Light-Harvesting Antennas of Photosynthetic Purple Bacteria by Stark Spectroscopy. 1. LH1 Antenna Complex and the B820 Subunit from *Rhodospirillum rubrum*

Lucas M. P. Beekman,[†] Martin Steffen,[§] Ivo H. M. van Stokkum,[†] John D. Olsen,[‡] C. Neil Hunter,[‡] Steven G. Boxer,[§] and Rienk van Grondelle^{*,†}

Department of Physics & Astronomy, Vrije Universiteit, De Boelelaan 1081, 1081 HV Amsterdam, The Netherlands; Krebs Institute for Biomolecular Research and Robert Hill Institute for Photosynthesis, Department of Molecular Biology and Biotechnology, University of Sheffield, Sheffield S0 2TN, U.K.; and Department of Chemistry, Stanford University, Stanford, California 94305-5080

Received: November 4, 1996; In Final Form: April 3, 1997[⊗]

We present low-temperature Stark measurements on the core light-harvesting complex 1 (LH1) of purple bacteria and the B820 subunit derived from LH1, which is a protein bound Bchl *a* dimer. It was found that the B820 dimer exhibits only a small Stark signal dominated by a difference dipole moment between ground and excited states, $|\Delta\mu| \cong 1.4$ D/f. The B820 complex can be reassociated to form LH1-like (B873) complexes, and this aggregation process induces a dramatic increase in the Stark parameters; $|\Delta\mu| \cong 3.7$ D/f and $\text{Tr}(\Delta\alpha) \cong 1300\text{--}1800$ Å³/f². No significant differences were found between the B873 complex and the native LH1 antenna. The electrooptic properties of LH1 are compared to those of the special pair of the reaction center and the peripheral antenna complex, LH2, and discussed in the context of the ringlike structures observed for bacterial light-harvesting complexes. It is argued that the strong Stark signal of LH1 arises from mixing of charge transfer states with the exciton states of closely interacting pigments, the smallest possible unit being a Bchl *a* dimer. The absence of a strong Stark signal in B820 is most likely due to a small structural rearrangement of the protein bound dimer and the loss of interactions with neighboring pigments compared to the case of LH1.

Introduction

The photosynthetic light-harvesting antenna absorbs light energy and transfers the excitation energy with high efficiency to the photosynthetic reaction center (RC). The light-harvesting system in photosynthetic purple bacteria generally consists of a core antenna surrounding the RC, usually referred to as the light-harvesting 1 antenna, LH1, or B875, since the bacteriochlorophyll *a*, Bchl *a*, molecules within LH1 absorb maximally at approximately 875 nm. In some bacteria, the LH1 antenna is surrounded by a peripheral LH2 or B800-850 antenna. In this arrangement the excitations are directed toward the RC where they are trapped and drive a charge separation. Eventually, the energy is stabilized by a series of secondary electron transfer steps: for a review see ref 1.

The light-harvesting antenna systems of most purple bacteria consist of a basic unit containing two small polypeptides, α and β , each with a molecular mass of about 5 kDa. Both α and β span the membrane once, and a highly conserved histidine (His) residue, within each of these transmembrane α -helices, binds a Bchl *a* molecule near the periplasmic side of the photosynthetic membrane.^{2,3} These histidines serve as a fifth ligand for the central magnesium of the Bchl *a* molecules.⁴ Furthermore, it has been proposed that within the basic building block of the antenna, the $\alpha\beta$ -subunit, the Bchl *a* molecules are organized in dimers and that the $\alpha\beta$ -subunits assemble in rotationally symmetric complexes.^{2,3,5}

Recently, the high-resolution structure for the LH2 complex of *Rhodospseudomonas (Rps.) acidophila* was obtained, which

reveals a ringlike structure.⁶ In this LH2 the $\alpha\beta$ -building blocks form a ring with 9-fold rotational symmetry. The nine α -subunits are on the inside and the nine β -subunits on the outside with the 18 B850 Bchls sandwiched between the two concentric rings. The distances between the central magnesium atoms, Mg, of the Bchl *a* molecules are on the order of 9 Å. Relatively small differences in distance are found between neighboring Bchl *a* molecules on adjacent dimers and within a dimer.^{6,7} For LH2 of *Rhodospirillum (Rsp.) molischianum*, an $\alpha_8\beta_8$ complex with a very similar arrangement of the pigments and proteins was obtained.⁸ Furthermore, based on a low-resolution (8.5 Å) projection map of the LH1 complex of *Rsp. rubrum*,⁹ a circular aggregate was proposed that exhibits a 16-fold rotational symmetry. The similarities of protein sequence and spectral and structural features suggest that the structure of LH1 strongly resembles that of LH2. We will therefore often refer to the LH2 structure as a model for LH1 and discuss the results in terms of this structure.

The photosynthetic purple bacterium *Rsp. rubrum* contains only the core antenna complex (LH1); exposure of membranes of *Rsp. rubrum* to 1% β -octylglucoside (β -OG) dissociates the LH1 complex into smaller complexes with a main absorption feature at 820 nm. This complex will be further referred to as B820.^{10–12} By reducing the detergent concentration, the B820 complexes can be reassociated to form a complex absorbing at 873 nm at room temperature, B873. Further increasing the β -OG concentrations of the B820 sample results in the formation of a broad absorption band around 777 nm, B777.^{10–12}

The B820 complex has been thoroughly characterized using a variety of spectroscopic methods and was found to be a dimer of two Bchl *a* molecules, bound to an α - and β -polypeptide pair.^{12–15} The reassociation of B820 into B873 yields a complex that spectroscopically is very similar to LH1.^{12,16} The B777

[†] Vrije Universiteit.

[‡] University of Sheffield.

[§] Stanford University.

* To whom correspondence should be addressed.

[⊗] Abstract published in *Advance ACS Abstracts*, August 15, 1997.

complex is most probably a monomer Bchl *a* molecule bound to either of the two polypeptides. Resonance Raman spectroscopy shows that the central magnesium molecule in the Bchl *a* molecule is still 5-ligated, indicating the ligation to the His residue is still present.¹⁷

The most conspicuous observation upon reassociating the monomers, B777, to form B873 is the red shift of almost 100 nm. This red shift is most probably due to both pigment–pigment and pigment–protein interactions. Upon dissociation of LH1 into B820, a loss of a hydrogen bond to a C₂-acetyl carbonyl group is observed,¹⁴ which reappears upon reassociation to B873. However, single hydrogen bonds are usually believed to only induce spectral shifts of at most 10 nm.^{18–20} Furthermore, for LH2 and LH1 it was concluded from site directed mutagenesis experiments that the formation or breaking of a hydrogen bond to a C₂-acetyl carbonyl of the Bchl *a* molecules fine-tunes the position of the absorption maxima.^{18–21} Pigment–pigment interactions are dominated by excitonic interactions, which may induce large spectral shifts. For the strength of the excitonic interaction the geometry of the pigments in the complex plays an important role. From the LH2 structure both the intradimer and interdimer exciton couplings are estimated to be similar and around 300 cm⁻¹.^{22,23} Furthermore, intradimer charge transfer (CT) character could influence the spectrum of the B820 dimer and the LH1 and LH2 complexes. For instance, the large red shift of the special pair dimer (P) absorption band of the RC has been explained by assuming that P is a strongly exciton coupled dimer in which CT character is mixed into the lowest exciton state.²⁴

To study the nature and relative importance of the different interactions that contribute to the spectral properties of LH1, we have performed electric field (Stark) effect measurements on the various LH1-type pigment protein complexes of *Rsp. rubrum* and *Rhodobacter (Rb.) sphaeroides*. In previous work the Stark signal of LH1 complexes from *Rb. capsulatus* was measured; the values found for the Stark parameters were 3.3 D/f for the difference dipole moment, $|\Delta\mu|$, and for the difference polarizability $\text{Tr}(\Delta\alpha) > 1000 \text{ \AA}^3/f$.²⁵ An attempt was made to explain the results obtained in terms of a dimeric model for LH1. Within the model of the dimeric nature of LH1 the red shift up to 875 nm should result either from the creation of strong excitonic interactions between the pigments or, alternatively, from CT states mixing into the lowest exciton state, inducing a large red shift as was concluded for P. However, CD spectroscopy suggests a rather weak exciton coupling between the pigments in LH1,²⁶ and $|\Delta\mu|$ was found to be smaller than observed in P.²⁵ This did not agree with the apparent relation between the red shift of the absorption bands and $|\Delta\mu|$. The $|\Delta\mu|$ value obtained for the LH1 absorption band was smaller than what would be expected on the basis of the spectral red shift.

Here we report the Stark spectra of B820, B777, B873, and of the native LH1 complex. We show that the large polarizability of LH1 is a property of the LH1 ring and not of the purified B820 $\alpha\beta$ -Bchl *a*₂ heterodimer. We discuss the spectral properties of LH1 in light of these results and the available structural information.

Materials and Methods

The experimental setup was similar to the one described previously in ref 25. The Stark cell consisted of two indium tin oxide (ITO) coated glass plates glued together with double-sided sticky tape, which also served as a spacer, resulting in cells with a thickness of approximately 100 μm . The ITO coating is both optically transparent (>95%) and conducts

electric current, which provides the opportunity to perform optical experiments and to apply an electric field across the sample at the same time. The high-voltage supply was a home-built high-voltage amplifier, preamplified by a hi-fi amplifier. The internal oscillator of an EG&G Model 5210 lock-in amplifier was used to drive the high-voltage with a modulation frequency of approximately 300 Hz, and the detection of the lock-in amplifier was set to the double frequency, $2f$. We measured the dependence of the Stark signal on the angle between the electric field vector of the light and the applied electric field, χ , by putting the cell at a fixed angle $\sim 35^\circ$ – 45° and turning the polarization direction of the incident light.

Stark spectra were measured on LH1 complexes from a *Rb. sphaeroides* mutant M2192²⁷ and on B873, B820, and B777 complexes isolated from *Rsp. rubrum*. M2192 is a RC⁻ LH2⁻ strain of *Rb. sphaeroides*; membranes were isolated as described in ref 27. Chromatophores from the carotenoid-less *Rsp. rubrum* mutant G9 were solubilized in a solution of *n*-octyl- β -D-glucopyranoside (β -OG).^{10–14} All samples were mixed with glycerol to a 50:50 (v/v) ratio. All measurements were performed at 77 K in a liquid N₂ cryostat in which the sample space was also filled with liquid N₂.

For these Stark experiments, an OD of at least 0.1 per $\sim 100 \mu\text{m}$ was required in order to obtain an absorption spectrum of reasonable quality. For ordinary steady-state absorption or fluorescence measurements the concentration of the sample can be a factor of 10–100 lower. Due to the high concentration of the B820 complexes and the very small volumes ($\sim 40 \mu\text{L}$) required for these experiments, it was impossible to make spectroscopically “pure” B820 or B777 samples. Therefore, we have performed a series of measurements on samples with a range of detergent concentrations that as a result varied the contribution of each of the different spectral forms. The absorption spectra obtained for all samples were analyzed globally using skewed Gaussian line profiles²⁸ to obtain the minimum number of spectral species that could reasonably describe the absorption data. The skewed Gaussian line profile is given by

$$\epsilon(\nu) = \exp \left[-\ln 2 \left\{ \frac{\ln \left(1 + 2b \frac{\nu - \nu_{\max}}{\Delta\nu} \right)}{b} \right\}^2 \right] \quad (1)$$

with parameters ν_{\max} (location), $\Delta\nu$ (width), and b (skewness). The extra skewness parameter allows a reasonable description of most species with a single band. The parameters for the absorption profiles obtained from this fit were used as the starting parameters in the analysis of the Stark spectra.

The spectral response of randomly oriented and spatially fixed molecules to an externally applied electric field^{29,30} is given in eq 2.

$$\Delta A(\nu) = (f\mathbf{F}_{\text{ext}})^2 \left\{ A_\chi A(\nu) + \frac{B_\chi}{15hc} \left(\frac{\nu d[A(\nu)/\nu]}{d\nu} \right) + \frac{C_\chi}{30h^2c^2} \left(\frac{\nu d^2[A(\nu)/\nu]}{d\nu^2} \right) \right\} \quad (2)$$

In eq 2, \mathbf{F}_{ext} is the externally applied electric field and f is the local field correction factor which relates the applied electric field to the electric field at the site of the molecule. All terms A_χ , B_χ , and C_χ are dependent on the macroscopic angle between the polarization direction of the light and the electric field, χ . The second derivative contribution to the Stark effect yields information on the difference dipole moment between the ground and the excited state of the molecule, $\Delta\mu$. From the

dependence of the second derivative contribution on χ the angle, ζ , between $\Delta\mu$ and the transition dipole, \mathbf{p} , can be found; see eq 3. Furthermore, for the difference polarizability tensor (between the ground and excited state), $\Delta\alpha$, the χ dependence yields the ratio of the projection of $\Delta\alpha$, on \mathbf{p} and the trace of the $\Delta\alpha$ tensor (eq 4). The size of this ratio is indicative of the orientation of $\Delta\alpha$ with respect to \mathbf{p} . Thus, the dependence of the Stark signal on the macroscopic angle χ gives information about the molecular orientation of the Stark parameters $\Delta\mu$ and $\Delta\alpha$. For C_χ and B_χ the following relations hold:^{29,30}

$$C_\chi = |\Delta\mu|^2 \{5 + (3 \cos^2 \chi - 1)(3 \cos^2 \zeta - 1)\} \quad (3)$$

$$B_\chi = \frac{1}{2} \text{Tr}(\Delta\alpha) \left\{ 5 + (3 \cos^2 \chi - 1) \left(3 \frac{\mathbf{p} \cdot \Delta\alpha \cdot \mathbf{p}}{\text{Tr}(\Delta\alpha)} - 1 \right) \right\} \quad (4)$$

The factor working on the zeroth derivative in eq 2, A_χ , has a similar $3 \cos^2 \chi - 1$ angle dependence as B_χ and C_χ (eqs 3 and 4). This term describes the effect of the electric field on the oscillator strength of the optical transition studied. It contains information on the transition polarizability and transition hyperpolarizability,^{29,30} which determine the field dependence of \mathbf{p} .

In the analysis of a Stark spectrum, $\Delta A(\nu)$, the absorption and Stark spectrum were fitted simultaneously with respectively a number of skewed Gaussian bands and the second, first, and zeroth derivative of these Gaussian bands. Instead of skewed Gaussians, we have also used other line shapes to fit the spectra with comparable results both in terms of the values of $\Delta\mu$ and $\text{Tr}(\Delta\alpha)$ as in terms of the spectra. This analysis was repeated for each individual angle χ and yielded the angle dependence of the first and second derivative. The angle dependence of the second and first derivative were fitted to eqs 3 and 4, respectively. In this way the value for ζ and $\mathbf{p} \cdot \Delta\alpha \cdot \mathbf{p} / \text{Tr}(\Delta\alpha)$ were obtained.

Results

Absorption Spectra. Low-temperature (77 K) absorption spectra of the B873, B820, and B777 complexes as measured in the Stark cell are shown in Figure 1; each panel represents a different β -OG concentration. As mentioned above, due to the relatively high concentration of protein and Bchl *a* in these samples, much larger amounts of β -OG had to be added compared to previously reported concentrations.¹² This was also observed during resonance Raman experiments which, as in our case, required both high β -OG and Bchl *a* concentrations.^{14,31} Furthermore, because of the high concentrations and small volumes, it was not possible to obtain a sample of pure B777 or B820. Only B873 could be prepared in the Stark cell without contributions from the other complexes. In preparing a sample with mainly B777, large amounts of β -OG were required, which severely restricted the amount of pigment-protein complex that could be added, resulting in a low OD.

The quality of the absorption spectra measured in the Stark cell is rather poor, even under optimal conditions. Therefore, all absorption spectra were fitted simultaneously to a set of skewed Gaussians.²⁸ The result of this fit is also presented in Figure 1. In fitting the Stark spectra, we use the parameters obtained in this way as starting values and allow for only moderate changes in them during the simultaneous fitting procedure of Stark and absorption spectra. Note that the spectra of each preparation were fitted separately.

B820 Stark Spectra. In Figure 2, the 77 K absorption and Stark spectrum of a sample containing mainly B820 is shown together with the first and second derivative of its absorption

spectrum. To reduce the noise, the derivatives were calculated from a fit to the absorption spectrum. The first thing to note is that this particular sample contained not only B820 but also a small amount of B777. Before we discuss the simultaneous fit of Stark and absorption spectrum, it is instructive to take a closer look at the spectra in Figure 2.

According to eq 2, a Stark spectrum contains contributions that scale with the second-, first-, and zeroth-derivative spectra of the absorption spectrum. At first glance the Stark spectrum of B820 strongly resembles the second-derivative spectrum, which means that the Stark parameters are dominated by $\Delta\mu$. If a value for $|\Delta\mu|$ is estimated using only the second derivative, we obtain $|\Delta\mu| \cong 2 \text{ D/f}$. There are, however, notable differences between the Stark spectrum and the second-derivative spectrum. First of all, the second derivative is narrower than the Stark spectrum, and furthermore the positive features on the blue and red of the main negative peak are more apparent in the former spectrum. This suggests that also the first- and zeroth-derivative spectra contribute to the Stark spectrum. However, the maxima in the absorption spectrum and the minima in the Stark and second-derivative spectra are all at approximately the same wavenumber. This implies that the contribution of the first derivative, $\Delta\alpha$, to the Stark spectrum is small. A large first-derivative contribution would have manifested itself by a shift of the extremes of the Stark spectrum with respect to those of the second-derivative and absorption spectrum.

The exclusion of a first-derivative contribution leaves the possibility of a zeroth-derivative contribution, i.e., a field-induced loss of absorbance, combined with the second derivative as a reasonable description of the Stark spectrum. Adding the right amount of negative zeroth derivative to the second derivative yields a spectrum that has its extreme at the peak of the absorption, a broadened negative lobe, and a reduction of the intensity of the positive features on the blue and red side, relative to those in the second-derivative spectrum.

As mentioned in the previous section, we have analyzed the Stark spectra using a computer program in which eq 2 was implemented and have fitted the absorption and Stark spectra simultaneously with a series of skewed Gaussian profiles and the latter spectra with the derivatives of these Gaussians. The results of the fit for the B820 sample, discussed above, are shown in Figure 3. As was already pointed out in the qualitative discussion above, we obtain a reasonable fit of the data with only the second and zeroth derivatives contributing to the Stark spectra. The results of the fits are listed in Table 1.

B873 and LH1 Stark Spectra. The fits to the data for the B820 sample show mainly a second-derivative, some negative zeroth-derivative, and almost no first-derivative contribution. A completely different result, however, is obtained in case of reassociated B873 and M2192 membranes. In Figure 4 a,b the absorption, Stark, and derivative spectra of the two samples are shown. The strong similarity between the two sets of spectra is striking and can be taken as an indication that indeed B873 is reconstituted to a structure that in terms of Stark spectroscopy is very similar to the original LH1 structure. In both cases the Stark spectrum is clearly dominated by a first-derivative line shape. However, the Stark spectrum is slightly red-shifted with respect to the calculated first derivative. A similar effect is observed in the Stark spectra of LH2 complexes.^{21,25} In terms of eq 2 this red shift of the Stark spectrum, with respect to the first derivative, most likely arises from a second-derivative contribution.

The Stark and absorption spectra of these complexes have also been fitted simultaneously. The result for M2192 is shown

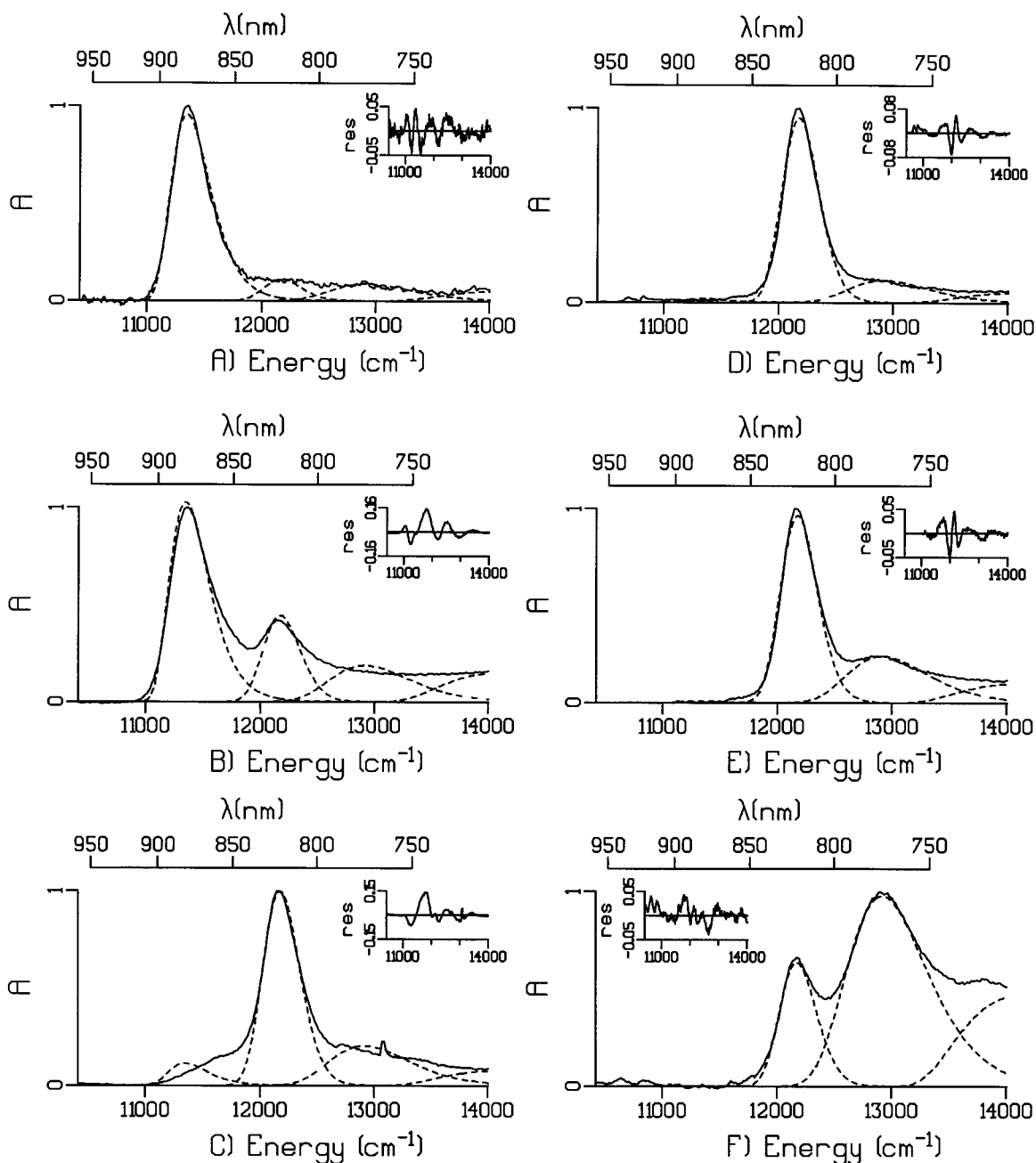


Figure 1. In panels A–F absorption spectra as measured in the Stark cell are displayed of samples with a gradually increasing detergent concentration. The spectra were simultaneously fitted with a set of four skewed Gaussian bands, given by the dashed curves, accounting for the B777, B820, and B873 complexes; the fourth band accounts for base line effects. The inset shows the residual of the fit. In panel C on the red side of the main 820 nm band there is a very poor fit to the spectrum. The samples were mixed always with 50% (v/v) of glycerol, and the other 50% was a mixture of a highly concentrated B820 stock solution and a buffer solution containing 15% β -OG. The ratios 15% β -OG:B820 stock solution as used for panels A–F were respectively 0:50, 13:37, 20:30, 25:25, 30:20, and 37:13. However, in the latter, panel F, the β -OG concentration in the stock solution was increased to be saturated, approximately 25% (w/v), to obtain a large amount of B777.

in Figure 5; the main contribution to the Stark spectrum is the first derivative and corresponds to a value for $\text{Tr}(\Delta\alpha)$ of $\sim 1800 \text{ \AA}^3/\text{f}^2$. From the fit estimates for the second- and zeroth-derivative are also obtained, and the results are listed in Table 1.

B777. Figure 6 shows Stark and absorption spectra of a preparation in which the highest possible amount of B777 was reached compared to the amount of B820. The quality of both absorption and Stark spectra is poor due to the low absorption of the sample. However, since the negative peaks in the Stark spectra coincide with the position of the absorption bands, we conclude that the main contributions from B777 and B820 to the Stark spectrum of this sample are second derivative, suggesting that both signals are dominated by $\Delta\mu$. We have

fitted the Stark and absorption spectrum simultaneously using three skewed Gaussian profiles: two for spectral forms present in the sample, B777 and B820, and the third to account for the base line effects arising from the poor quality of the absorption spectrum. Contributions of the first derivative were not incorporated in the fit because of the poor quality of both absorption and Stark spectra. The use of only the zeroth and second derivative in the fit can be justified by the fact that free Bchl *a* in solution³² is dominated by $\Delta\mu$, and as is shown above also the Stark spectrum of B820 lacks a first-derivative contribution. The values obtained from this fit are also listed in Table 2. The main observation from this sample is the larger $|\Delta\mu|$ value for B777 compared to that for B820. Note that the resulting $|\Delta\mu|$ for B820 in this sample is very similar to that

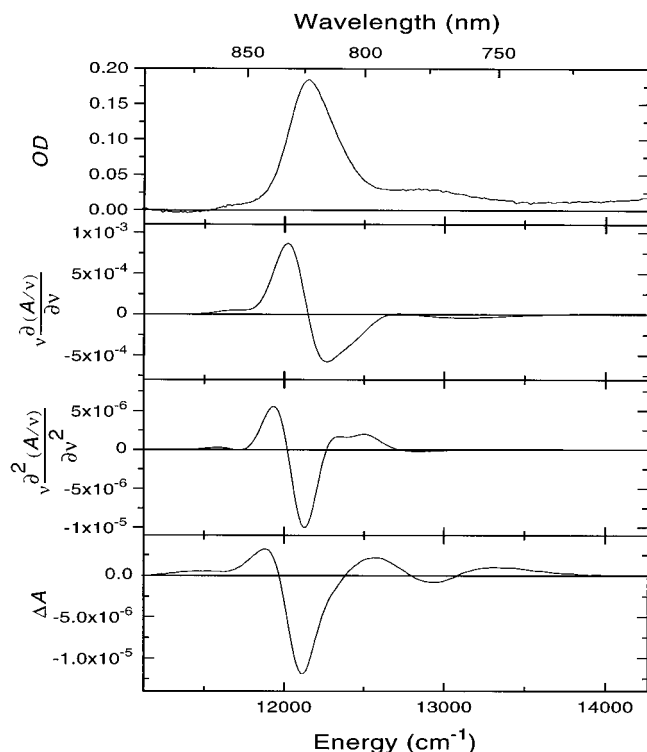


Figure 2. From top to bottom we show the 77 K absorption spectrum and first- and second-derivative spectra and the Stark spectrum of a preparation of B820. The Stark spectrum was measured at $\chi = 54.7^\circ$ and the electric field strength $F = 1.0 \times 10^5 \text{ V cm}^{-1}$. The derivative spectra were calculated from a fit to the absorption spectrum.

obtained for the more pure B820 preparation discussed above; see Figures 2 and 3. The analysis of both preparations yields a $|\Delta\mu|$ value for B777 that is about twice as large as $|\Delta\mu|$ found for B820.

Angle Dependence Measurements. The contributions of the fitted first- and second-derivative spectra to the Stark spectra as a function of the angle between the electric field vector of the linearly polarized light and the applied electric field χ yield information about the orientation of the microscopic parameters $\Delta\mu$ and $\Delta\alpha$ with respect to the transition dipole \mathbf{p} (eqs 3 and 4). In Figure 7 the angle dependencies of C_χ and B_χ are shown for M2192, B873, and B820. For the second-derivative term the dependence on χ gives us information about the angle between the transition dipole \mathbf{p} and the difference dipole $\Delta\mu$, ζ . From our data we estimate ζ to be small, which means that the difference dipole is oriented mainly along the optical transition dipole moment. We have listed the estimated angles in Table 2.

Understanding the angle dependence of the first-derivative contribution is slightly more complicated. Since $\Delta\alpha$ is a tensor, we cannot define an angle as is done for $\Delta\mu$, where ζ is defined as the angle between two vectors. However, we can give an estimate of the projection of the tensor, $\Delta\alpha$, on the transition dipole (eq 4: $\mathbf{p} \cdot \Delta\alpha \cdot \mathbf{p} / \text{Tr}(\Delta\alpha)$) and therefore give an indication of how large the component of the polarizability tensor is along the transition dipole. The points of the first-derivative contributions lead to estimates of $\mathbf{p} \cdot \Delta\alpha \cdot \mathbf{p} / \text{Tr}(\Delta\alpha)$ on the order of 0.9–0.95. So the principal axis of the difference polarizability tensor in M2192 and B873 is found to make an angle with the transition dipoles of approximately 10° – 20° . These results are also listed in Table 3.

In Table 1 we have furthermore listed the Stark parameters obtained for isolated RCs. These RCs were isolated from membrane bound RC-only membranes, which allows for a much

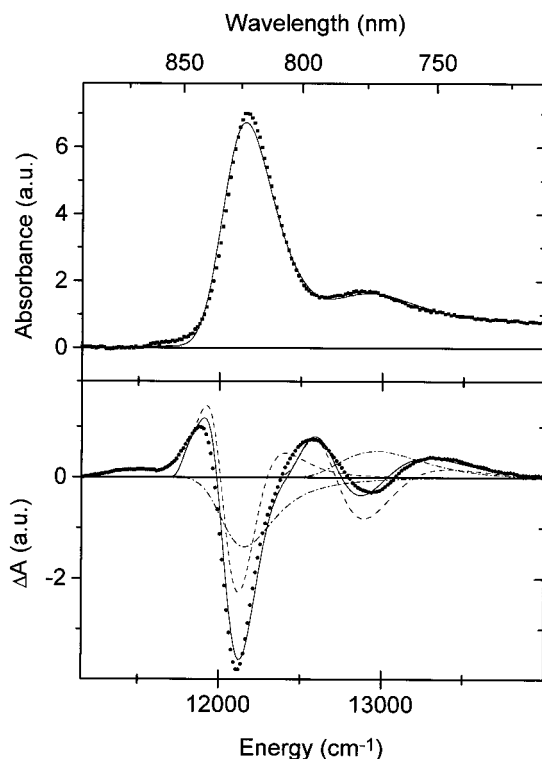


Figure 3. Simultaneous fit of absorbance (top) and Stark spectra (bottom) of a B820 preparation to eq 2. The points represent the data and the drawn line the fit, the same data are shown as in Figure 2. In fitting the Stark spectrum, only the second and zeroth derivative contribute. If a first derivative is allowed, a small negative first-derivative contribution is found for the B820 complex, $\text{Tr}(\Delta\alpha) = -50 \text{ \AA}^3/f^2$. This negative first derivative may be an artifact arising as a result of the presence of impurities in the sample, i.e., B777. In the lower figure the second derivative (dash) and zeroth derivative (dash dot) of the spectral components are given in their relative contributions to the Stark spectrum.

TABLE 1: Values for the Stark Parameters Obtained from the Simultaneous Fit of Absorption and Stark Spectra of Different Preparations

sample	λ (nm)	A_χ (cm^2/kV^2)	$\text{Tr}(\Delta\alpha)$ ($\text{\AA}^3/f^2$)	$ \Delta\mu $ (D/f)
B777	773			4.0(1.0)
B820	822	-53×10^{-10}	$-50(10)$	1.4(0.1)
B873 (20-11-95)	880	-128×10^{-10}	1300(90)	3.8(0.1)
M2192 (LH1 only)	884	-189×10^{-10}	1800(100)	3.5(0.1)
RC (P-band)	888	-151×10^{-10}	1150(80)	5.2(0.1)

milder isolation procedure.³³ The obtained value for $|\Delta\mu|$ is the same, i.e., 5.2 D/f, as that reported in ref 29, while $\text{Tr}(\Delta\alpha)$ is slightly higher: $1150 \text{ \AA}^3/f^2$ compared to $930 \text{ \AA}^3/f^2$.

Discussion

Upon dissociation of LH1 into its subunit B820, we observe that both the amplitude and the line shape of the Stark spectrum undergo dramatic modifications. The line shape changes from almost pure first derivative for LH1 and B873 to second derivative for B820. The Stark signal of LH1 and B873 is dominated by $\Delta\alpha$, demonstrating that the excited state of the complex is highly polarizable. Upon dissociation of these structures into B820, the polarizability is almost completely lost. Further dissociation of B820 into the protein bound Bchl *a* monomer B777 produces a further change in the Stark spectrum observed as an increase in $|\Delta\mu|$.

The LH1 and B873 Stark Spectra. The Stark spectra of B873 and LH1 from M2192, in Figure 4, are very similar. In both cases the first-derivative line shape dominates although it

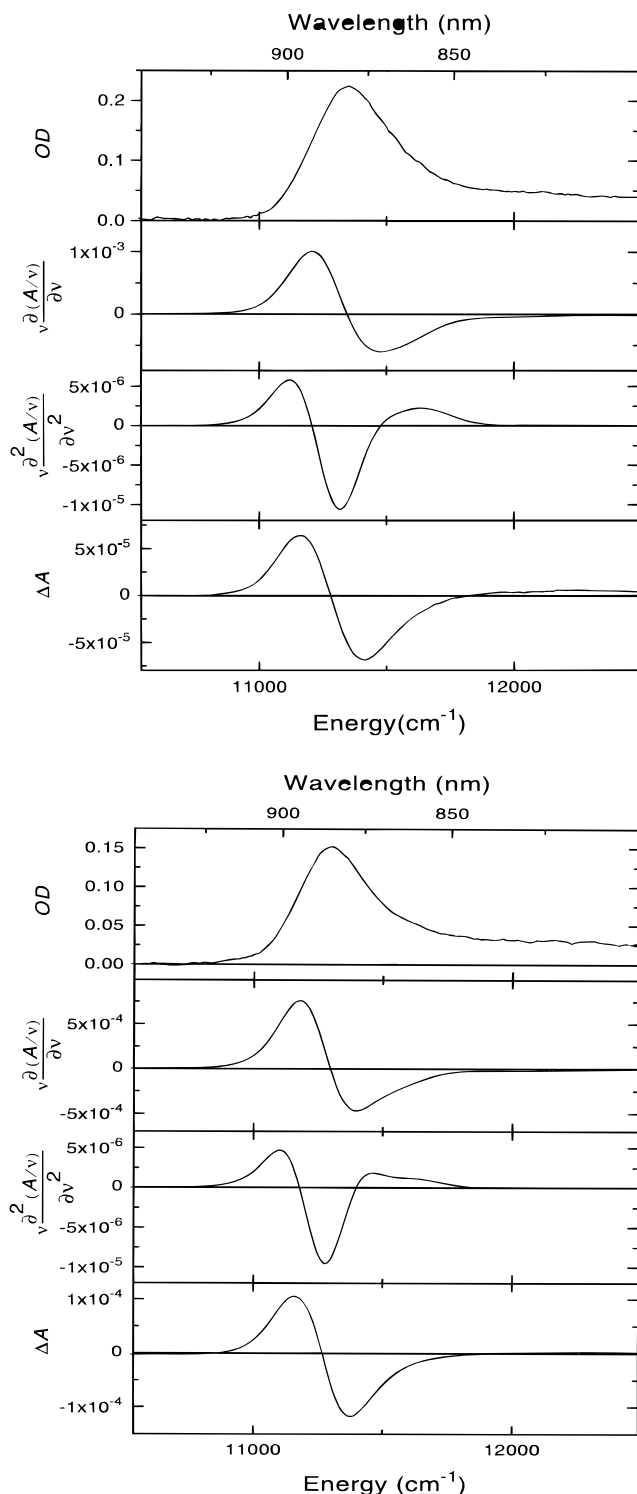


Figure 4. The 77 K absorbance-, first derivative-, second derivative-, and Stark spectra measured at $\chi = 54.7^\circ$ and at a field strength of $F = 1.0 \times 10^5 \text{ V cm}^{-1}$ of (A) M2192 and (B) reconstituted B873 complexes.

is clearly red-shifted with respect to the calculated first derivative. Also, the estimated Stark parameters of both complexes are similar as can be seen in Table 1 and Table 2. This is a further indication that the complex formed upon reassociation of B820 strongly resembles the native LH1.

Both B873 and M2192 have a high value for $\text{Tr}(\Delta\alpha)$ (1300 and $1800 \text{ \AA}^3/f^2$, respectively). These $\text{Tr}(\Delta\alpha)$ s are of a similar magnitude as that reported by Gottfried et al. for LH1 complexes from *Rb. capsulatus*. A large $\text{Tr}(\Delta\alpha)$ is also observed for the special pair, P, of the bacterial RC,^{29,32} although this value is about 40% lower than that of LH1. The resemblance of the

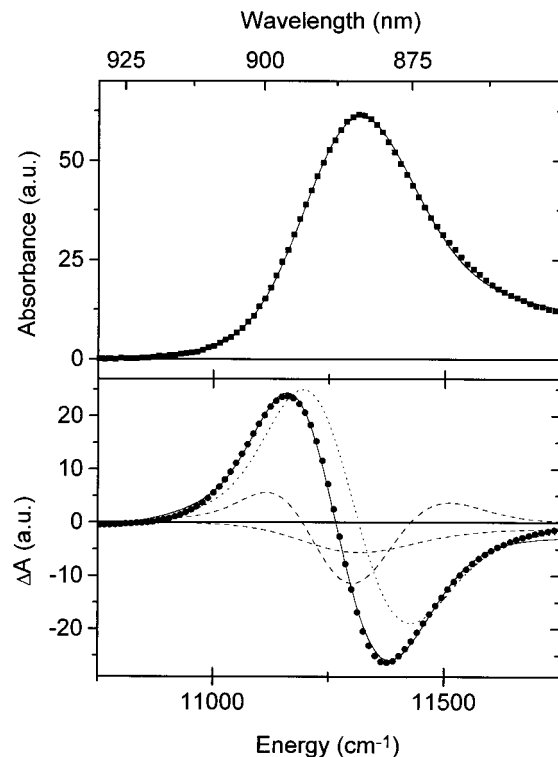


Figure 5. Simultaneous fit of absorbance (top) and Stark spectra (bottom) of M2192 (see also Figure 4A). Data are represented as points, the fit is given by the drawn lines. The absorption spectrum is fitted by a sum of two skewed Gaussian profiles. The resulting band was treated as a single absorption profile in calculating the derivatives and fitting the Stark spectrum; i.e., the ratio of the amplitudes of the two bands was the same for Stark and OD spectra. In the Stark spectrum the contributions of the second (dashed), first (dotted), and zeroth (chain-dot) derivative are plotted. The signal is clearly dominated by the first derivative, and smaller contributions of the second and zeroth derivative are found. The obtained values for $|\Delta\mu|$ and $\text{Tr}(\Delta\alpha)$ are given in Table 2.

spectral and electrooptic properties of P and LH1 suggests a common origin. For P the remarkable electrooptic properties have been explained in terms of the mixing of a charge transfer (CT) state with the lowest excitonic state, most likely an intradimer CT state. Furthermore, in the presence of a matrix field (due to the protein), a difference dipole is induced. In LH1, similar to P, Bchl *a* molecules are strongly excitonically coupled and closely packed. Whether or not the spectroscopic unit is also a dimer is not entirely clear. However, for simplicity of the discussion, we will follow this approach. We propose that the electrooptic properties of LH1 have the same origin as those of P, i.e., a charge transfer state mixed with the lowest exciton state spanned by minimally a dimer of Bchl *a* molecules. Since the basic spectroscopic unit of LH1 is also a dimer,^{10–17} we propose that the electrooptic properties of LH1 have the same origin as those of P, i.e., a charge transfer state mixed with the lowest exciton state. A similar explanation is proposed for the electrooptic properties of LH2.²¹ In the LH2 structure there is continuous electron density between the Bchls associated with an $\alpha\beta$ -subunit.⁶

It is not clear how the neighboring pigments in the LH1 (and LH2) ring and in the RC contribute to the observed electrooptic properties. In the RC the angle between \mathbf{p} and $\Delta\mu$, ζ , and the angle between \mathbf{p} and the principal axis of $\Delta\alpha$ were found to be similar as the angle between \mathbf{p} and the axis connecting P and B_L (or B_M).²⁹ For LH1 this angle is 11° for B873 and 18° for M2192 (Table 2). In a 16-fold symmetric ring, the angle between the transition dipole of a dimer with the vector connecting the two adjacent dimers is 11° , supporting the idea

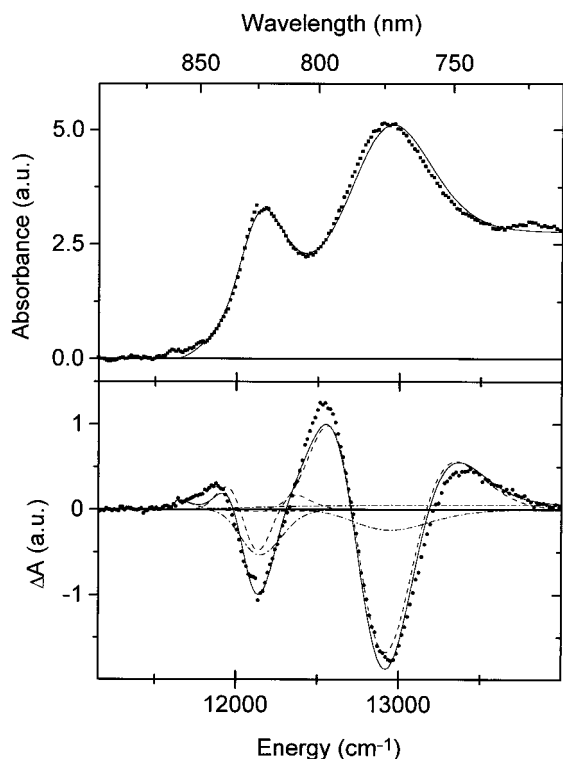


Figure 6. Absorbance (upper) and Stark (lower) spectra of a preparation with mainly B777; see also Figure 1, panel F. The spectra are fitted with three skewed Gaussians, of which the second (dash) and zeroth (dash dot) derivatives contribute to the fit of the Stark spectrum. The values for B820 are $|\Delta\mu| = 1.4$ D/f and $A_\chi = -60 \times 10^{-10}$, and for B777 the values are $|\Delta\mu| = 4.0$ D/f and $A_\chi = -19 \times 10^{-10}$ cm² kV⁻².

TABLE 2: Values for ζ and $\mathbf{p} \cdot \Delta\alpha \cdot \mathbf{p} / \text{Tr}(\Delta\alpha)$ Obtained from the χ Dependence of the Stark Signal

species	
B820 $\Delta\mu$	$\zeta = 13^\circ$
B873 $\Delta\mu$	$\zeta = 8^\circ$
B873 $\Delta\alpha$	$\mathbf{p} \cdot \Delta\alpha \cdot \mathbf{p} / \text{Tr}(\Delta\alpha) = 0.96$ ($\zeta = 11^\circ$)
M2192 $\Delta\mu$	$\zeta = 2^\circ$
M2192 $\Delta\alpha$	$\mathbf{p} \cdot \Delta\alpha \cdot \mathbf{p} / \text{Tr}(\Delta\alpha) = 0.90$ ($\zeta = 18^\circ$)

that the neighboring pigments in the ring contribute to the increased polarizability.

The larger value of $|\Delta\mu|$ found for P compared to that for LH1 is most likely due to differences in the protein matrix field, $\mathbf{F}_{\text{matrix}}$, which results from charged amino acid residues.

In ref 34 the electric field effect properties of a circular aggregate, similar to the LH2 structure, are studied within the framework of exciton interactions.^{23,35} From this work it was concluded that the large Stark effect of LH1 and LH2 cannot be explained by exciton interactions only. Other pigment–pigment interactions, specifically CT, should be included to come close to a proper description.

B820 Stark Spectrum. The Stark spectrum of B820 is weak and is dominated by $\Delta\mu$, whereas $\text{Tr}(\Delta\alpha)$ is found to be close to zero. Furthermore, in the fit a negative contribution from a zeroth derivative is required. The values of $|\Delta\mu|$ and $\text{Tr}(\Delta\alpha)$ in B820 are much smaller than observed for LH1 and LH2^{21,25} and in particular the values obtained for P in the bacterial RC.^{25,29}

Many of the spectroscopic properties of B820 have suggested a structural resemblance with P or with the dimer of the $\alpha\beta$ -subunit in LH2.^{6–8} The differences between the three are as follows: First of all, P and the LH2 dimers are completely surrounded by protein and other pigments, while B820 is most

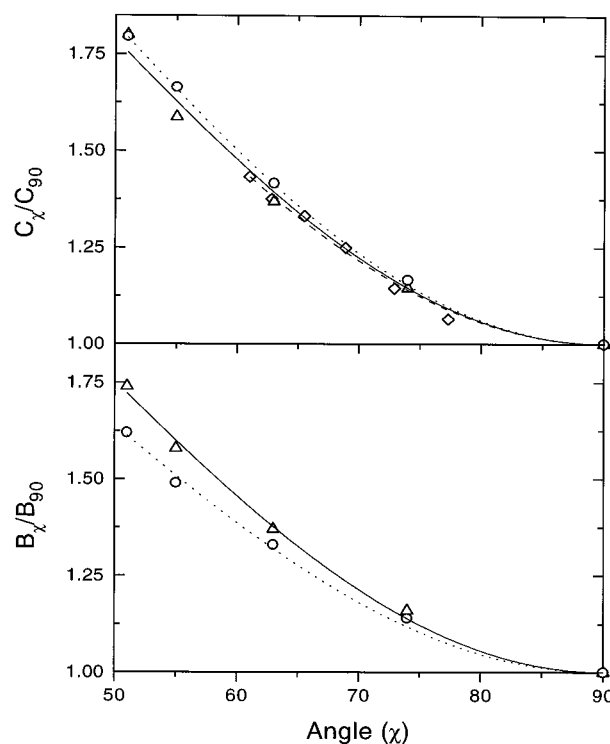


Figure 7. χ Angular dependence of second-derivative (upper panel) and first-derivative (lower panel) contributions to the Stark spectra of B820 (diamonds), B873 (triangles), and M2192 (circles) is shown. The points are the contributions of the second and first derivative, obtained from the fits, at each experimental angle χ , divided by the contribution at $\chi = 90^\circ$. The data points are fitted to quotient of C_χ/C_{90} , eq 3 (top panel), and B_χ/B_{90} , eq 4 (lower panel), which yields respectively an estimate of ζ and $\mathbf{p} \cdot \Delta\alpha \cdot \mathbf{p} / \text{Tr}(\Delta\alpha)$. The χ dependence of C_χ/C_{90} yields $\zeta \sim 10^\circ$; the values per sample are listed in Table 3. The lower panel shows B_χ/B_{90} ; the estimated $\mathbf{p} \cdot \Delta\alpha \cdot \mathbf{p} / \text{Tr}(\Delta\alpha)$ ratios for are around 0.95 (see also Table 3).

likely partly exposed to detergent. This difference in the surrounding medium between P and B820 may influence the local electric field experienced by the dimers. Furthermore, the distance between the central Mg atoms in the Bchl *a* molecules is about 7 Å in P, about 9 Å for the dimer in the LH2 structures, and possibly even larger for B820.³⁶ We will try to explain the fact that the Stark parameters are different in B820 as compared to P and the LH2 dimer, bearing in mind the above-mentioned structural differences.

Both P and LH2/1 exhibit a large value of $\text{Tr}(\Delta\alpha)$ in contrast to B820. For P and also for LH1/2 this interpreted as due to the mixing of CT states with the lowest exciton state of the dimers. Apparently this does not happen in B820. As a consequence, the Stark parameters for B820 are similar to those for the Bchl *a* protein from *Prosthecochloris aestuarii*.²⁵ Stark spectra of these complexes are dominated by $\Delta\mu$, with values on the order of 1.5–2.3 D/f.²⁵ Although the pigments are found to be strongly exciton coupled based on CD spectroscopy,³⁷ the Stark properties are those of a monomer. Thus, we conclude that B820 is an excitonically coupled dimer of two Bchl *a*'s, which in terms of Stark spectroscopy have conserved their monomeric properties.

In fitting the B820 Stark spectrum, there is a clear requirement for a zeroth-derivative contribution to the Stark spectrum, although usually the zeroth-derivative contribution is small and can be neglected. However, we should point to the fact that also for P the zeroth derivative contributes significantly.²⁹ Moreover, a zeroth-derivative contribution was required for B873 and M2192, in order to fit the Stark spectrum properly (see Figure 5). Therefore, we believe that the main reason for

the zeroth-derivative contribution being so explicitly required in the description of the Stark spectrum for B820 is simply the very low $|\Delta\mu|$ and $\text{Tr}(\Delta\alpha)$ values rather than an excessively large loss of oscillator strength. This conclusion can also be arrived at from the values given for A_z of the different samples in Table 1.

A Structural Change in B820 upon the Formation of LH1.

To explain the low $\Delta\alpha$ of B820, we suggest a slight deformation of the dimer upon the isolation of B820. In the absence of a high-resolution structure of B820 and LH1, we will use spectroscopic data, results from mutagenesis, and the LH2 crystal structure to discuss the possible structural differences between B820 and LH1. In LH2 a His residue serves as the fifth ligand for the central magnesium in the Bchl *a* molecule.⁶⁻⁸ The conservation of these histidines in the protein sequences of LH2 and LH1, and the observation from Raman spectroscopy that the Mg is 5-coordinate, and recent mutagenesis data (Olsen et al., manuscript in preparation) demonstrate that this is also the case in LH1.^{4,17} Replacing this His residue on the β -polypeptide by an Asn results in LH1 complexes with a relatively normal absorption band.^{38,39} Resonance Raman data, however, show that a hydrogen bond to a C₉-keto of the Bchl *a* molecule is lost in the mutant complex.^{38,39} This suggests that apart from serving as a ligand for the central magnesium the His residue also has a structural role in forming a hydrogen bond to a C₉-keto of an adjacent Bchl. In the crystal structure of LH2 the C₉-keto group of the Bchl *a*'s are within hydrogen-bonding distance to the His residues, which serve as a ligand to the central Mg of the other Bchl *a* in the dimer. Note that in LH2 this H bond is not formed.^{6,8} The resonance Raman spectrum of B820 has shown that the hydrogen bonds to the C₉-keto groups were slightly weakened in B820 compared to LH1 and B873,¹⁴ indicating a change in distance between the groups.

Furthermore, from Fourier transform (FT) resonance Raman spectroscopy, it has been concluded that the C₂-acetyl of one Bchl *a* molecule in LH1 is involved in a hydrogen bond with the tryptophan (Trp) residue on the α -subunit 11 residues away from the ligating His toward the C-terminus (αTrp_{+11})²⁰ and the other C₂-acetyl group forms a hydrogen bond to βTrp_{+9} (Sturgis et al., submitted). Upon dissociation of LH1 into B820, a hydrogen bond to a C₂-acetyl is lost, which reappears after reassociation to B873.¹⁴ The B820 complex from the $\alpha\text{Trp}_{+11}\rightarrow\text{Phe}$ mutant has no shift in absorption maximum, but reconstitution to B873 gives the expected ~ 20 nm blue shift.⁴⁰ A combination of this knowledge of the hydrogen bonds with other data should facilitate the construction of a simplified model for the LH1 structure.

Judging from these data, we suggest that the B820 dimer is probably slightly distorted with respect to the native structure as found in LH1. This might lead to an increased center-to-center distance between the Bchl *a* molecules from about 9 Å in the native structure to about 11 Å in B820,³⁶ resulting in a decreased overlap of the electron densities. The loss of overlap of the electron density might also result from a slight rotation or other distortion of B820 upon isolation.

Intermediates in the Reassociation. In Figure 8 we have plotted the Stark spectra of four different preparations that were made with various amounts of detergent. As is clearly observed, the samples are mixtures of B820 and other spectral forms on the red side with a large Stark effect strongly resembling B873. However, as the relative contribution of the long-wavelength species increases, the spectrum shifts further to the red. Most typical for this effect are the latter two spectra, represented by solid and dashed lines in Figure 8. A clear, ~ 10 nm, red shift

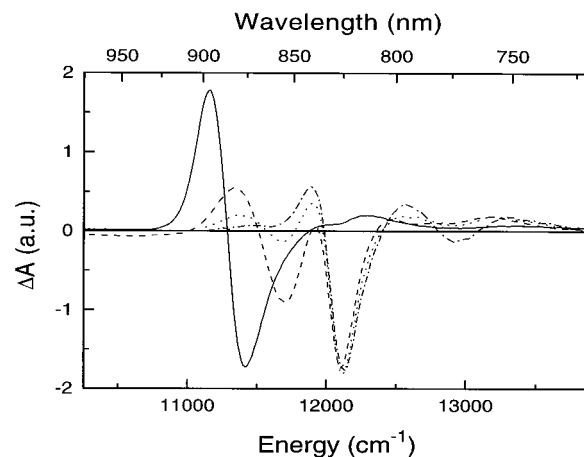


Figure 8. Stark spectra of preparations with different concentrations of detergent are shown, the spectra are scaled arbitrarily to present them in one picture. The absorbance spectra corresponding to these Stark spectra are shown in Figure 1: dash-dot, panel E; dot, panel D; dash, panel C; solid, panel B. The shift of the zero crossing of the red feature in the two latter spectra is indicative for the presence of intermediate complexes between B820 and B873.

is observed when increasing the amounts of B873-like complexes. This suggests that upon the reassociation intermediate complexes are formed. These intermediates have a red-shifted spectrum with respect to B820, but are not shifted as far as B873, and furthermore their Stark effect is already large. This contrasts with earlier observations in stopped flow experiments which suggest that no intermediate spectral forms were required to fit the reassociation reaction of B820 to B873.¹⁵ Another indication for a spectral intermediate can be taken from Figure 1. The absorption spectrum in panel C of Figure 1 is clearly not well fitted on the red side by the band that accounts for the B873 contribution; a more blue-shifted band seems much more appropriate.

The fact that in the case of the intermediate complexes the Stark signals are already extremely large and of a first-derivative-like shape suggests that most of the electrooptic properties are already contained by the intermediates. There are two effects that should occur upon aggregation. First, the B820 dimer should become more compact, resulting in the reappearance of the electron density overlap between the two Bchl *a*'s. And strengthening of the hydrogen-bonds to the C₉-keto's. A second effect is the stacking of the dimers in a particular ring-shaped structure, resulting in the re-formation of a H-bond to one of the C₂-acetyls,¹⁴ the reappearance of strong interactions with neighboring pigments, and possibly even an increase of the spectral unit from a dimer to larger multimers. These effects are all expected to result in a spectral red shift and to affect the electrooptic properties of the complexes. Furthermore, recent data suggest that a complete ring may not be necessary to obtain the red shift to about 875 nm.⁴¹

There may be several reasons for the observation of these intermediates in our experiments. Since the Stark effect of the intermediate spectral forms is much larger than of B820, their signal will appear in Stark spectroscopy even when they are not visible using other spectroscopic techniques. Furthermore, the high concentration of detergent and protein, the small volumes, and the fact that the samples are frozen relatively quickly after being prepared, therefore stopped at some intermediate state in the equilibration process, may have resulted in larger relative contributions of the intermediate complexes.

B777 Stark Spectrum. In the two preparations with significant contributions of B777 (Figures 2, 3, and 6) $|\Delta\mu|$ is found to be significantly larger in B777 than in B820. Although

we cannot make a conclusive statement about the exact size of $|\Delta\mu|$, we estimate it to be about 1.5–2 times larger for B777 than for B820. $|\Delta\mu|$ of B777 is also larger than observed for free Bchl *a* in solution,³² which suggests that the Bchl *a* molecule in B777 is indeed protein bound, and the protein environment seems to significantly affect $|\Delta\mu|$.

Acknowledgment. The authors thank Drs. Jan-Adriaan Leegwater and Frank van Mourik for useful discussions. L.B. acknowledges support from the Dutch Foundation for Life Sciences. This work was supported by the EC Contracts CT92-0796 and CT93-0278 and the Human Frontier Science Program.

References and Notes

- (1) van Grondelle, R.; Dekker, J. P.; Gillbro, T.; Sundström, V. *Biochim. Biophys. Acta* **1994**, *1187*, 1–65.
- (2) Zuber, H. *TIBS* **1986**, *11*, 414–419.
- (3) Brunisholz, R. A.; Zuber, H. *J. Photochem. Photobiol. B* **1992**, *15*, 113–140.
- (4) Robert, B.; Lutz, M. *Biochim. Biophys. Acta* **1985**, *807*, 10–23.
- (5) Hunter, C. N.; van Grondelle, R.; Olsen, J. D. *TIBS* **1989**, *14*, 72–76.
- (6) McDermott, G.; Prince, S.; Freer, A.; Hawthornthwaite-Lawless, A.; Papiz, M.; Cogdell, R. J.; Isaacs, N. W. *Nature* **1995**, *374*, 517–521.
- (7) Freer, A.; Prince, S.; Sauer, K.; Papiz, M.; Hawthornthwaite-Lawless, A.; McDermott, G.; Cogdell, R. J.; Isaacs, N. W. *Structure* **1996**, *4*, 449–462.
- (8) Koepke, J.; Hu, X.; Muenke, C.; Schulten, K.; Michel, H. *Structure* **1996**, *4*, 581–597.
- (9) Karrasch, S.; Bullough, P. A.; Ghosh, R. *EMBO J.* **1995**, *14*, 631–638.
- (10) Miller, J. F.; Hinchigeri, S. B.; Parkes-Loach, P. S.; Callahan, P. M.; Sprinkle, J. R.; Loach, P. A. *Biochemistry* **1987**, *26*, 5055–5062.
- (11) Chang, M. C.; Callahan, P. M.; Parkes-Loach, P. S.; Cotton, T. M.; Loach, P. A. *Biochemistry* **1990**, *29*, 421–429.
- (12) Visschers, R. W.; Chang, M. C.; van Mourik, F.; Parkes-Loach, P. A.; Heller, B. A.; Loach, P. A.; van Grondelle, R. *Biochemistry* **1991**, *30*, 2951–2960.
- (13) Visschers, R. W.; Van Mourik, F.; Monshouwer, R.; van Grondelle *Biochim. Biophys. Acta* **1993**, *1141*, 238–244.
- (14) Visschers, R. W.; van Grondelle, R.; Robert, B. *Biochim. Biophys. Acta* **1993**, *1183*, 369–373.
- (15) Van Mourik, F.; Corten, E. P. M.; Van Stokkum, I. H. M.; Visschers, R. W.; Kraayenhof, R.; Van Grondelle, R. In *Research in Photosynthesis*; Murata, N., Ed.; Kluwer Academic Publishers: Dordrecht, 1992; Vol. 1, pp 101–104.
- (16) Van Mourik, F.; van der Oord, J. R.; Visscher, K. J.; Parkes-Loach, P. S.; Loach, P. A.; Visschers, R. W.; van Grondelle, R. *Biochim. Biophys. Acta* **1991**, *1059*, 111–119.
- (17) Sturgis, J. N.; Robert, B. *J. Mol. Biol.* **1994**, *238*, 445–454.
- (18) Fowler, G. J. S.; Visschers, R. W.; Grief, G. G.; van Grondelle, R.; Hunter, C. N. *Nature* **1992**, *355*, 848–850.
- (19) Fowler, G. J. S.; Sockalingum, G. D.; Robert, B.; Hunter, C. N. *Biochem. J.* **1994**, *229*, 695–700.
- (20) Olsen, J. D.; Stockalingum, G. D.; Robert, B.; Hunter, C. N. *Proc. Natl. Acad. Sci. U.S.A.* **1994**, *91*, 7124–7128.
- (21) Beekman, L. M. P.; Frese, R. N.; Fowler, G. J. S.; Ortiz de Zarate, I.; Picorel, R.; Cogdell, R. J.; van Stokkum, I. H. M.; Hunter, C. N.; van Grondelle, R. *J. Phys. Chem. B* **1997**, *101*, xxxx.
- (22) Jimenez, R.; Dikshit, S. N.; Bradforth, S. E.; Fleming, G. R. *J. Phys. Chem.*, in press.
- (23) Sauer, K.; Cogdell, R. J.; Prince, S. M.; Freer, A.; Isaacs, N. W.; Scheer, H. *Photochem Photobiol.* **1996**, 564–576.
- (24) Lathrop, E. J. P.; Friesner, R. A. *J. Phys. Chem.* **1994**, *98*, 3056–3066.
- (25) Gottfried, D. S.; Stocker, J. W.; Boxer, S. G. *Biochim. Biophys. Acta* **1991**, *1059*, 63–75.
- (26) Kramer, H. J. M.; van Grondelle, R.; Hunter, C. N.; Westerhuis, W. H. J.; Amesz, J. *Biochim. Biophys. Acta* **1984**, *765*, 156–165.
- (27) Hunter, C. N.; van Grondelle, R.; van Dorssen, R. *J. Biochim. Biophys. Acta* **1989**, *973*, 383–389.
- (28) Van Stokkum, I. H. M.; Scherer, T.; Brouwer, A. M.; Verhoeven, J. W. *J. Phys. Chem.* **1994**, *98*, 852–866.
- (29) Middendorf, T. R.; Mazzola, L. T.; Lao, K.; Steffen, M. A.; Boxer, S. G. *Biochim. Biophys. Acta* **1993**, *1143*, 223–234.
- (30) Liptay, W. In *Excited States*; Lim, E. C., Ed.; Academic Press: New York, 1974; Vol. 1, pp 128–190.
- (31) Visschers, R. W. Personal communication.
- (32) Lao, K.; Moore, L. J.; Zhou, H.; Boxer, S. G. *J. Phys. Chem.* **1995**, *99*, 496–500.
- (33) Jones M. R.; Heer-Dawson, M.; Mattioli, T. A.; Hunter, C. N.; Robert, B. *FEBS Lett.* **1994**, *399*, 18.
- (34) Beekman, L. M. P. Thesis, Vrije Universiteit, Amsterdam, 1996.
- (35) Scherer, P. O. J.; Fischer, S. F. *Chem. Phys. Lett.* **1986**, *131*, 153–159.
- (36) Koolhaas, M. H. C.; van der Zwan, G.; van Mourik, F.; van Grondelle *Biophys. J.*, in press.
- (37) Pearlstein, R. M. *Photosynth. Res.* **1992**, *31*, 213–226.
- (38) Olsen, J. D. Thesis, University of Sheffield, 1994.
- (39) Olsen, J. D.; Sturgis, J.; Westerhuis, W. H. J.; Robert, B.; Hunter, C. N. Manuscript in preparation.
- (40) Davis, C. M.; Bustamante, P. L.; Todd, J. B.; Parkes-Loach, P. S., McGlynn, P.; Olsen, J. D.; McMaster, L.; Hunter, C. N.; Loach, P. A. *Biochemistry*, submitted.
- (41) Westerhuis, W. H. J.; Niedermann, R. A.; Hunter, C. N. Personal communication.